ELSEVIER

Polymer 41 (2000) 2391–2404

polymer

A structural study of (ethylene–vinyl alcohol) copolymers by high-resolution solid-state ^{13}C NMR

M. Kanekiyo[a], M. Kobayashi[a], I. Ando[a,*], H. Kurosu[b], S. Amiya[c]

[a]*Department of Chemistry and Materials Science, Tokyo Institute of Technology, Ookayama, Meguro-ku, Tokyo, Japan*
[b]*Department of Textile and Apparel Science, Nara Women's University, Kitauoya-Nishimachi, Nara, Japan*
[c]*Analytical Research Center, Kuraray Co., Ltd., Kurashiki, Okayama, Japan*

Received 21 December 1998; received in revised form 21 April 1999; accepted 26 May 1999

Abstract

High-resolution solid-state ^{13}C NMR spectra of (ethylene–vinyl alcohol) copolymers (EVOH) with various ethylene contents in the solid-state and their ^{13}C spin-lattice relaxation times, T_1, were measured, in order to elucidate the structure and dynamics of the copolymers. From these experimental results, the structural change of the EVOHs with changes of the ethylene content was successfully elucidated. Further, it is found that the ^{13}C T_1 for the CH carbon of the vinyl alcohol unit is mainly composed of two components. The fractions of short and long T_1 components increase and decrease with an increase in the ethylene fraction, respectively. From these experimental results, it can be said that changes of the ethylene content in the copolymers lead to large changes in their structure and dynamics.

Keywords: (Ethylene–vinyl alcohol) copolymer; Structure; Dynamics

1. Introduction

(Ethylene–vinyl alcohol) copolymer (EVOH) considered in this work consists of hydrophobic and hydrophilic parts which come from the vinyl alcohol (V) units and the ethylene (E) units, respectively. By changing their composition, EVOH can have specific properties such as a gas barrier. In order to understand the origin of such properties, it is very important to characterize the structure and dynamics of the copolymer. For this reason, the primary structure of the copolymers with a wide range of ethylene contents has been previously studied by high-resolution solution-state NMR [1–3]. In addition, the structure of copolymers in the solid-state has been studied by high-resolution solid-state NMR, which provides a powerful means of determining the structure and dynamics of solid polymers [4]. Nevertheless, some inconclusive assignments still remain due to the complicated structure of the copolymers, so that the V units often form intra and intermolecular hydrogen bonds with themselves, and the E units interact hydrophobically with themselves.

The structure and dynamics of poly(vinyl alcohol) (PVA) consisting of only V units and polyethylene (PE) consisting of only E units have been successfully studied by high-resolution solid-state ^{13}C NMR. As for PVA in the solid-state [5,6] and the gel-state [7–9], it has been shown that the CH carbon signal provides three split peaks, peaks I, II and III from downfield, which come from the CH carbons with two intra or intermolecular hydrogen bonds, one intra or intermolecular hydrogen bond, and no hydrogen bond, respectively. On the contrary, as for PE in the solid-state [10] it has been shown that in the crystalline region, two CH_2 carbon peaks corresponding to the orthorhombic and monoclinic crystallographic forms appear at about 33 and 34 ppm, respectively, in which the CH_2 carbons take the *trans* zigzag form and those in the noncrystalline region of the CH_2 carbons appear at about 30 ppm, which are undergoing fast transition between the *trans* and *gauche* conformations even at room temperature. From such a background, it is apparent that EVOH consisting of the V and E units has a complicated structure and dynamics.

In this work, we aim to make more detailed assignments of the observed high-resolution ^{13}C NMR spectra of EVOH in the solid-state with a wide range of ethylene contents, in addition to the previous assignments reported by Ketels, et al. [1,2] and VanderHart et al. [3], and to carry out the structural and dynamical characterization.

* Corresponding author. Tel.: +81-3-5734-2889; fax: +81-3-5734-2888.
E-mail address: iando@o.cc.titech.ac.jp (I. Ando)

0032-3861/00/$ - see front matter
PII: S0032-3861(99)00394-8

Table 1
Microstructure of EVOHs determined by solution ^{13}C NMR

Fraction/%										
Vinyl alcohol content	[V]	87	73	68	63	57	51	48	41	26
Ethylene content	[E]	13	27	32	37	43	49	52	59	73
Dyad	[V]	76.2	52.9	45.8	39.0	32.8	27.2	25.2	16.0	7.0
	[VE]	21.5	38.6	42.7	46.4	48.2	49.1	47.4	48.0	40.0
	[EE]	2.3	8.5	11.5	14.7	19.0	23.7	27.5	36.0	53.0
Triad	[VVV]	62.4	37.7	32.2	27.5	18.7	15.6	–[a]	–[a]	–[a]
	[VVE]	22.6	28.1	26.8	25.5	26.8	23.5	–[a]	–[a]	–[a]
	[EVE]	2.4	6.8	8.9	9.8	10.9	11.7	–[a]	–[a]	–[a]
	[VEV]	9.1	13.4	13.7	13.9	13.3	12.5	9.5	–[a]	–[a]
	[EEV]	3.0	11.8	14.6	17.8	22.4	25.3	22.6	–[a]	–[a]
	[EEE]	0.6	2.3	3.8	5.5	8.1	11.5	20.3	–[a]	–[a]
Block character[b] η		0.97	0.97	0.98	0.99	0.98	0.98	0.95	0.99	1.05

[a] Not determined with reasonable accuracy.
[b] Block character η is defined by $2f_V f_E/f_{VE}$, where f_V and f_E are the fraction of V and E units, and f_{VE} is the fraction of VE dyad.

2. Experimental section

2.1. Materials

The EVOH copolymers used in this work were obtained from Kuraray Co. Ltd., of which the ethylene contents are in the range of 5–94%. The glass transition temperature (T_g) of the EVOH samples, with ethylene contents ranging from 27 to 47% was determined by dynamic viscoelasticity method. The T_g for EVOHs with high ethylene content could not be

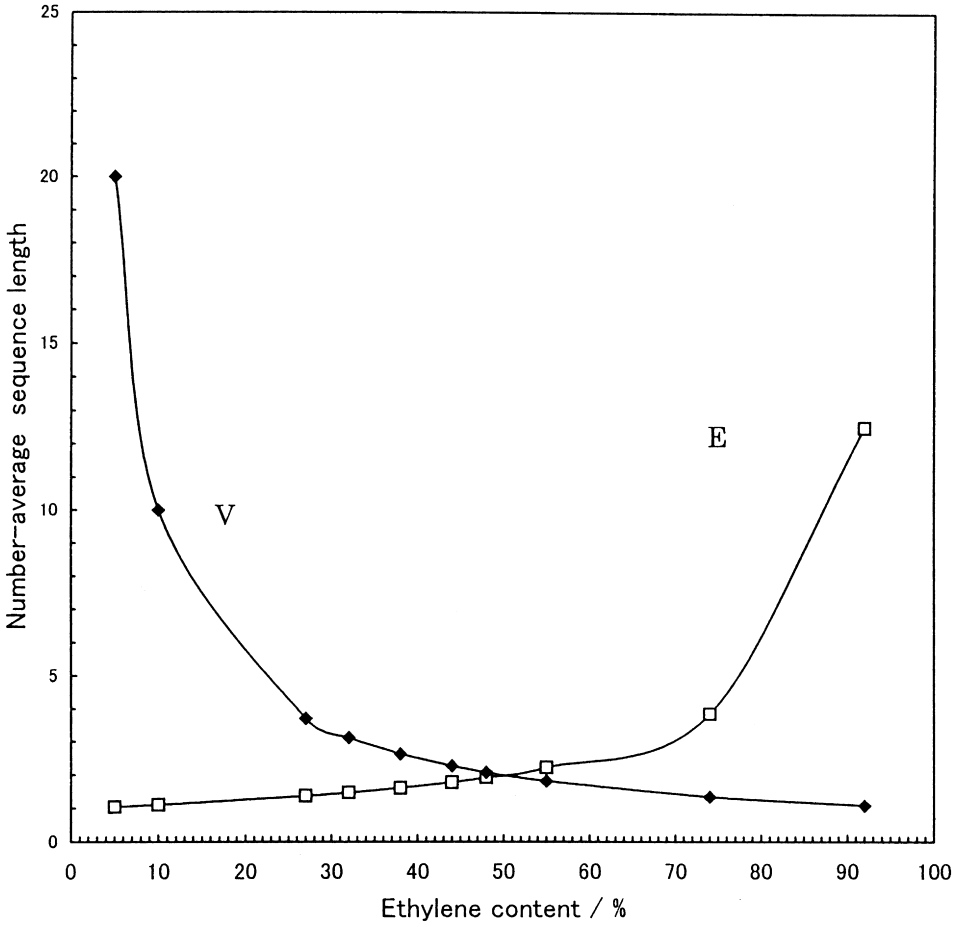

Fig. 1. Plots of the number-average ethylene and vinyl alcohol sequence length of EVOH against the ethylene content. □: ethylene sequence length; and ◆: vinyl alcohol sequence length.

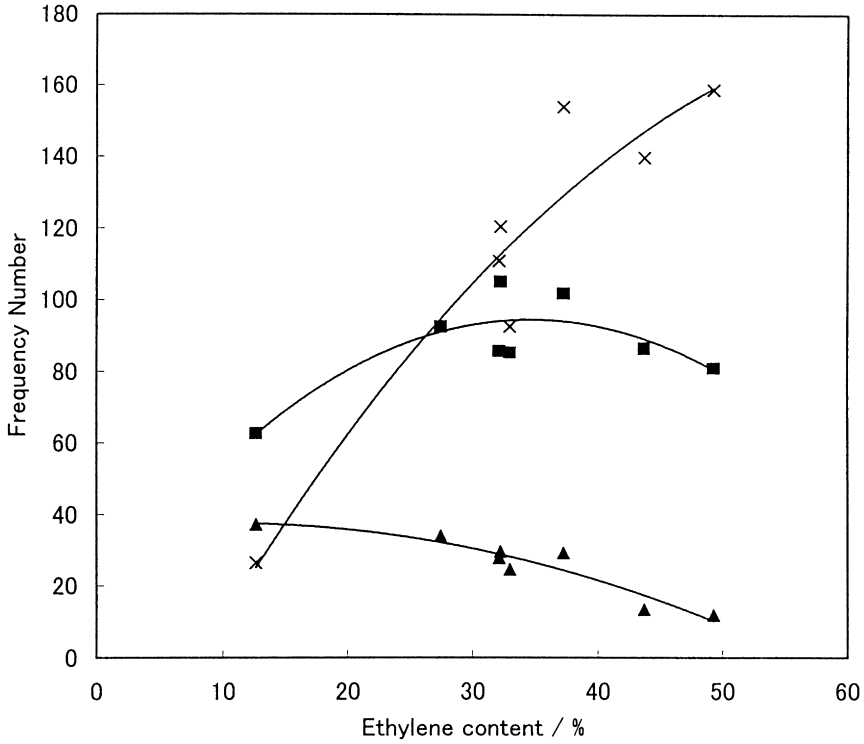

Fig. 2. Plots of the number of vinyl alcohol sequence length of EVOH against the ethylene content. ×: 1; ■: ≥2; and ▲: ≥8 for the vinyl alcohol sequence length.

determined with a high measure of reliability. It is expected that their T_gs are below room temperature.

The microstructure of these EVOH samples was characterized by solution-state ^{13}C NMR as shown in Table 1, where some EVOH samples with high ethylene content and triad fractions including the V unit could not be determined with high accuracy because of the very weak intensity of the corresponding peaks and hence are not listed.

2.2. High-resolution solid-state ^{13}C NMR measurements

High-resolution solid-state ^{13}C CP/MAS (cross polarization/magic angle spinning) [11–13] and ^{13}C PST/MAS (pulse saturation transfer/magic angle spinning) [14] NMR spectra were measured by a JEOL GSX-270 NMR spectrometer operating at 67.8 MHz. In the CP method, enhancement of the ^{13}C magnetization is effective for the relatively immobile components in solids and, on the contrary, in the PST method, the nuclear Overhauser effect (NOE) enhances the ^{13}C magnetization for the mobile component. The $\pi/2$ pulse widths for ^{1}H and ^{13}C nuclei are 4.9 and 5.5 ms, respectively. The contact time was 2 ms, and the repetition time was 5 s. The spectral width was 27 kHz and 8 k data points were taken. The spectra were accumulated 400–15 000 times to achieve a reasonable signal-to-noise ratio. The MAS rotor was spun at 3.8–4 kHz. The measurement temperature was about 45°C as indicated by the calibration temperature [15]. The ^{13}C chemical shifts were calibrated indirectly through the upfield peak (29.5 ppm) of adamantane relative to tetramethylsilane (TMS). The ^{13}C T_1 values were determined by the Torchia pulse sequence [16].

2.3. Markov-chain calculations for obtaining configurational sequences

The configurational structures of EVOH copolymers with various compositions of the E and V monomer units on the basis of the ^{13}C NMR spectral analysis and Markov-chain calculation can be characterized as reported already by Bruck [17] and Cheng et al. [18]. The structural characterization for analyzing the end groups of EVOH was carried out by the method of Moritani et al. [19]. The computer simulation for determining the sequence lengths was performed by 2nd-order Markov statistics [20] by using the dyad and triad fractions as shown in Table 1. These results will be used below when analyzing the ^{13}C chemical shift behavior of solid EVOH samples.

In the calculation, 10 000 Markov-chains with 1000 monomeric units were generated by computer. The calculations were performed on a Pentium II-266 MHz CPU machine.

3. Results and discussion

3.1. Markov-chain calculations

From the solution-state NMR experiments and Markov-chain calculations, the number-average sequence lengths of

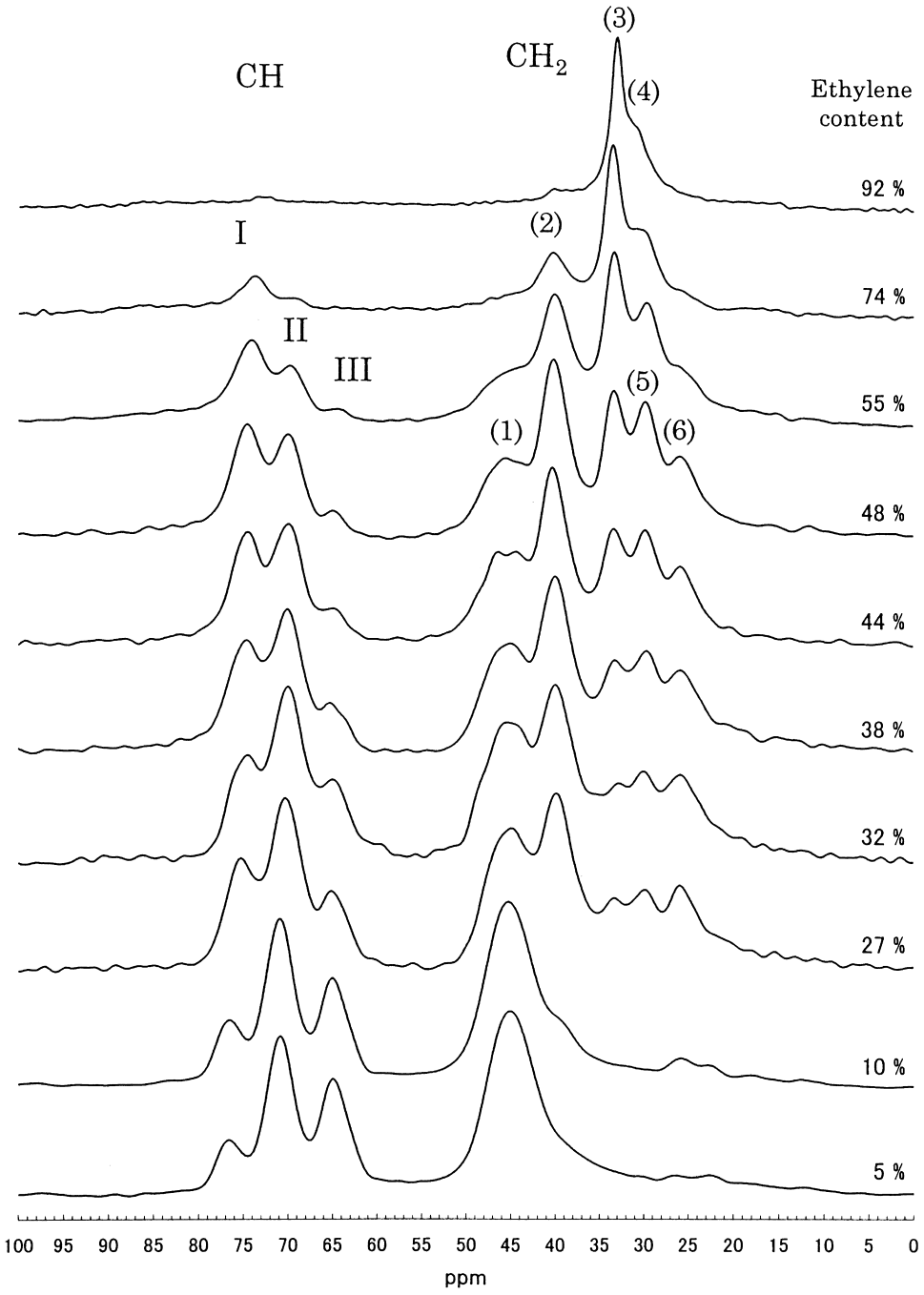

Fig. 3. 67.8 MHz ^{13}C CP/MAS NMR spectra of EVOH samples in the solid-state as a function of ethylene content.

the E and V units were obtained as a function of the ethylene content as shown in Fig. 1. It is found that as the fraction of the ethylene content (f_E) increases, the number-average sequence length of the E units increases slowly in the range of f_E ranging from 5 to 75%, and increases rapidly in the range of f_E larger than 75%. However, the number-average sequence length of the V units decreases rapidly as the ethylene content increases in the range from 5 to 25% and decreases slowly in the range larger than 25%. In Fig. 2 the frequency number of V unit sequences with 1, $\gtrsim$2 and 8 per 1000 monomer units is plotted against the ethylene content. It is found that as the ethylene content increases, the number of the V units that are 1 and $\gtrsim$8 increase and decrease, respectively, and those $\gtrsim$2 increase and has a maximum at an ethylene content of about 35%.

3.2. Solid-state ^{13}C NMR spectra and structural analysis

^{13}C CP/MAS NMR spectra of solid EVOH samples with a wide range of the ethylene contents at room temperature are shown in Fig. 3. The spectral patterns for the CH carbon of the V units and for the CH_2 carbon of the E and V units are

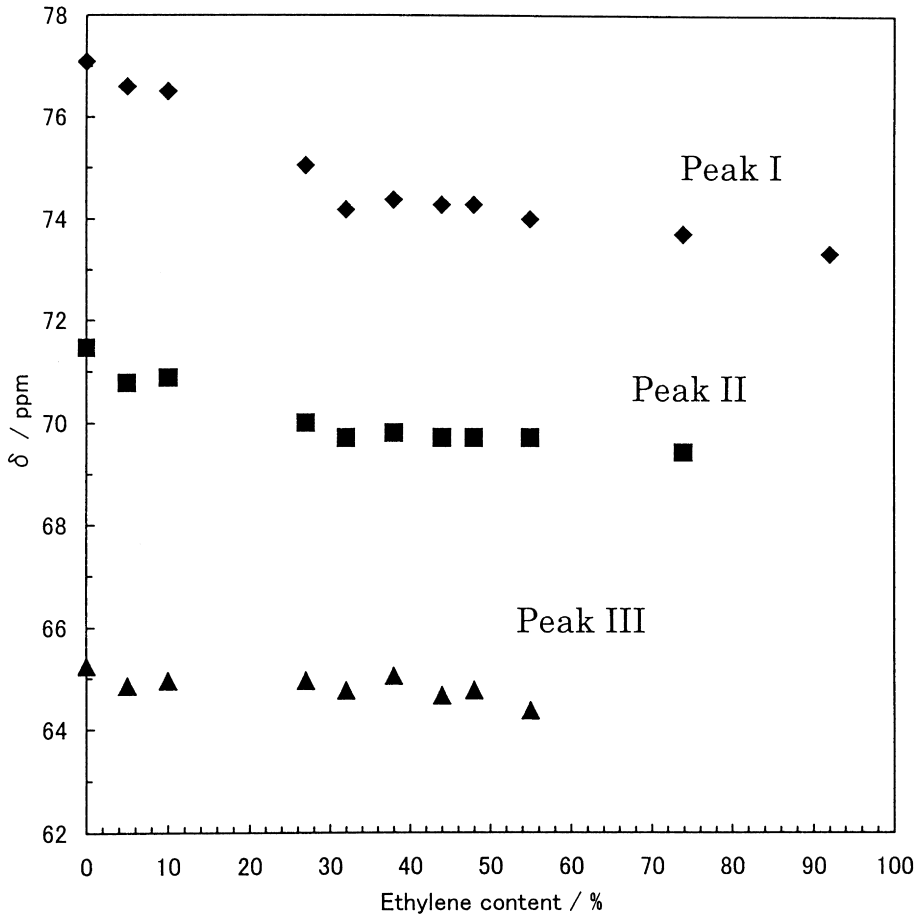

Fig. 4. Plots of the ^{13}C chemical shifts for the CH carbon of solid EVOH against the ethylene content as obtained by the ^{13}C CP/MAS experiments. ◆: peak I; ■: peak II; and ▲: peak III.

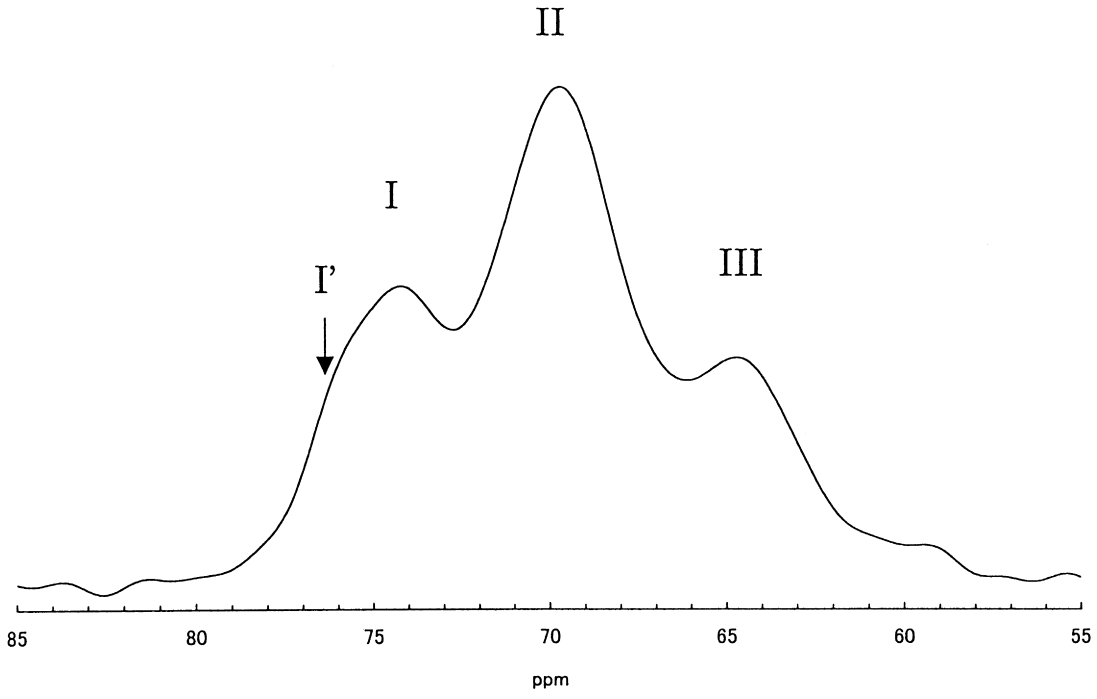

Fig. 5. Expanded 67.8 MHz ^{13}C CP/MAS NMR spectrum in the CH carbon region for EVOH in the solid-state with the ethylene content of 32%.

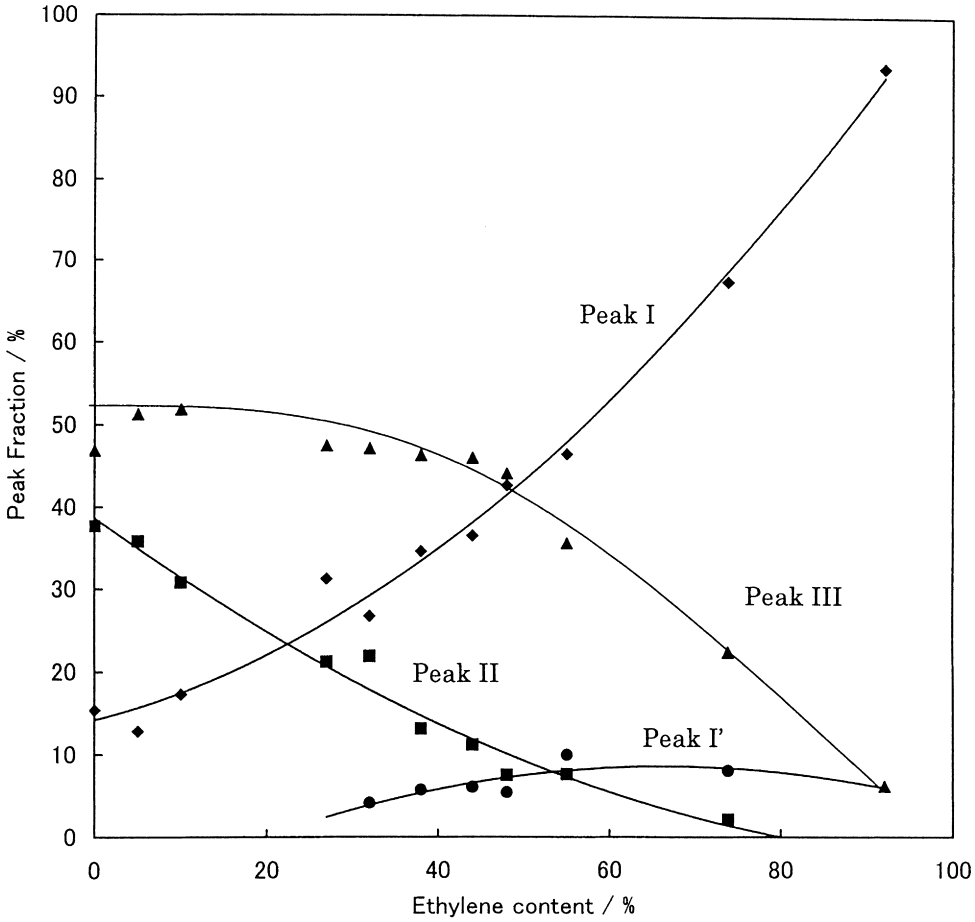

Fig. 6. Plots of the fractions of peaks I, II and III of the CH carbon for EVOH against the ethylene content. ●: peak I′; ◆: peak I; ■: peak II; and ▲: peak III.

greatly changed by varying the ethylene content. By using reference data from the solution ^{13}C NMR spectra of the corresponding samples and also the spectral change with changes of the ethylene content, the peak assignments of these spectra were made.

Three peaks of the CH carbon for consecutive V units appear in the range of 65–85 ppm. These three peaks correspond to those of solid PVA, which are named I, II and III from downfield. As reported in previous works on solid-state ^{13}C NMR studies of PVA gels [7–9], in addition to Teraos' [5] and Horiis' [6] works on solid-state ^{13}C NMR of PVA, peaks I (77 ppm), II (71 ppm) and III (65 ppm) come from the CH carbon with two intermolecular and/or intramolecular hydrogen bonds, one intermolecular or intramolecular hydrogen bond, and no hydrogen bond with the hydroxyl group, respectively. (The behavior in the fractions of peaks I, II and III for PVA in the gel state can be reasonably explained by considering the intramolecular hydrogen bond plus the intermolecular hydrogen bond. From such a consideration, we consider that the formation of one hydrogen bond leads to a downfield shift of about 6 ppm for the CH carbon in EVOHs in addition to the γ-gauche effect by CH_2 carbons as described below. Further, from the plots of the ^{13}C chemical shift positions for peaks I, II and III against the ethylene content as shown in Fig. 4, it is found that the position of peak III moves slightly upfield with an increase in the ethylene content, and the positions of peaks I and II move more largely upfield, compared with the case of peak III. At low ethylene contents, peak I consists of two overlapping peaks with a small difference in chemical shift as seen from the expanded signals for peaks I, II and III (Fig. 5). These two peaks are named as peaks I and I′ from downfield. The details of their assignments will be described below. In Fig. 6, the fractions of these peaks are shown as a function of the ethylene content. It is found that the fractions of peaks I and III increase and decrease, with an increase in the ethylene content, respectively, and the fraction of peak II is a constant in the range of ethylene content from 0 to 40% and decreases as the ethylene content is

Table 2
The glass transition temperature (T_g) of EVOHs with the ethylene contents from 27 to 47% as determined by dynamic viscoelasticity method

Fraction/%						
Vinyl alcohol content	[V]	73	68	62	56	53
Ethylene content	[E]	27	32	38	44	47
T_g/°C		72	69	62	55	50

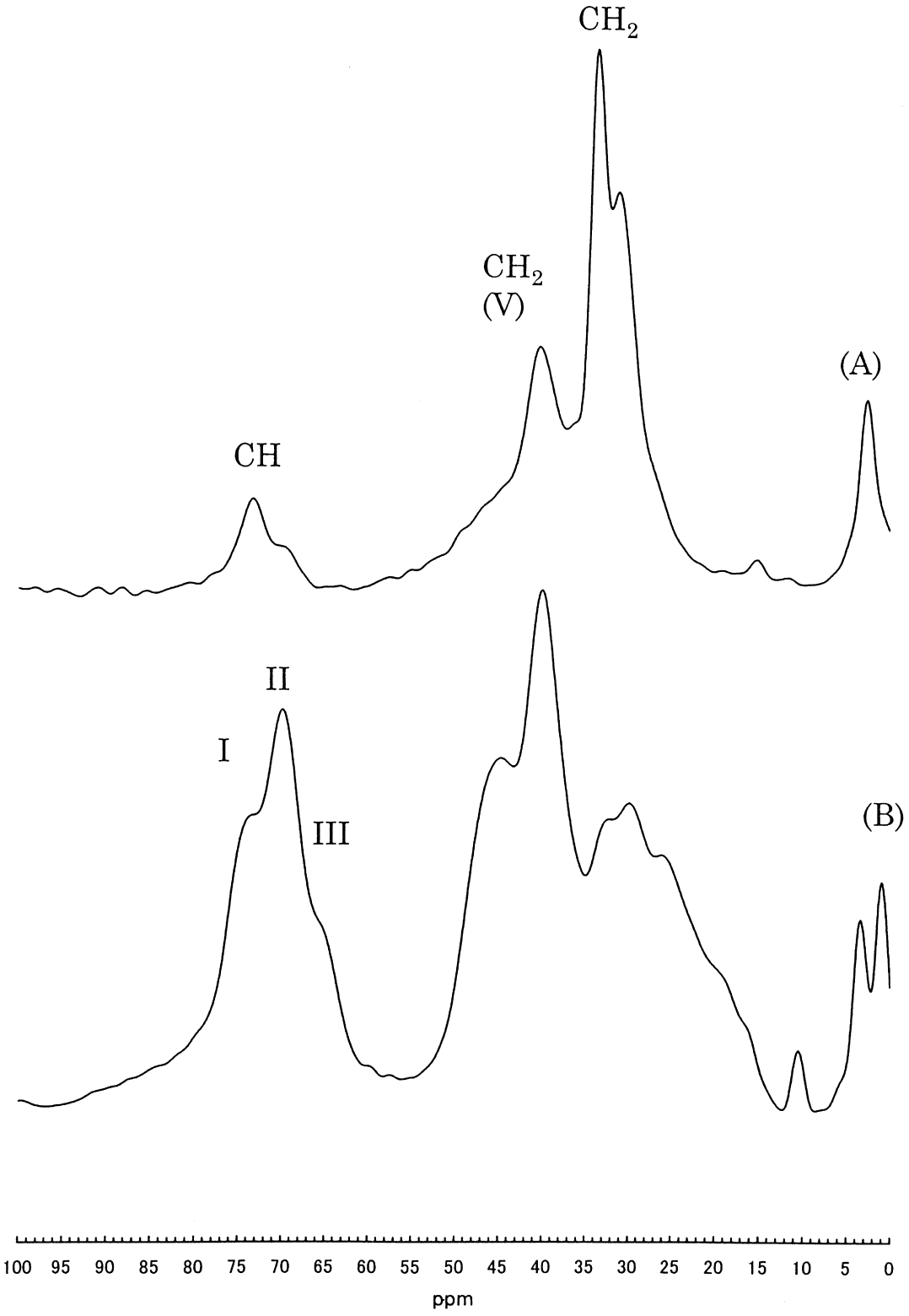

Fig. 7. 67.8 MHz ^{13}C PST/MAS NMR spectra of EVOH sample in the solid-state. (a) ethylene content: 74%. (b) ethylene content: 32%.

further increased. The fraction of peak I′ at about 77 ppm is slowly increased as the ethylene content is increased. At low ethylene contents, it was difficult to resolve peaks I and I′ as they overlapped each other even after computer fitting.

As reported previously [5,6], in the VV sequence, the *m* (*meso*) dyad will be able to form one intramolecular hydrogen bond and one intermolecular hydrogen bond, but the *r* (*racemic*) dyad will be able to form only one intermolecular

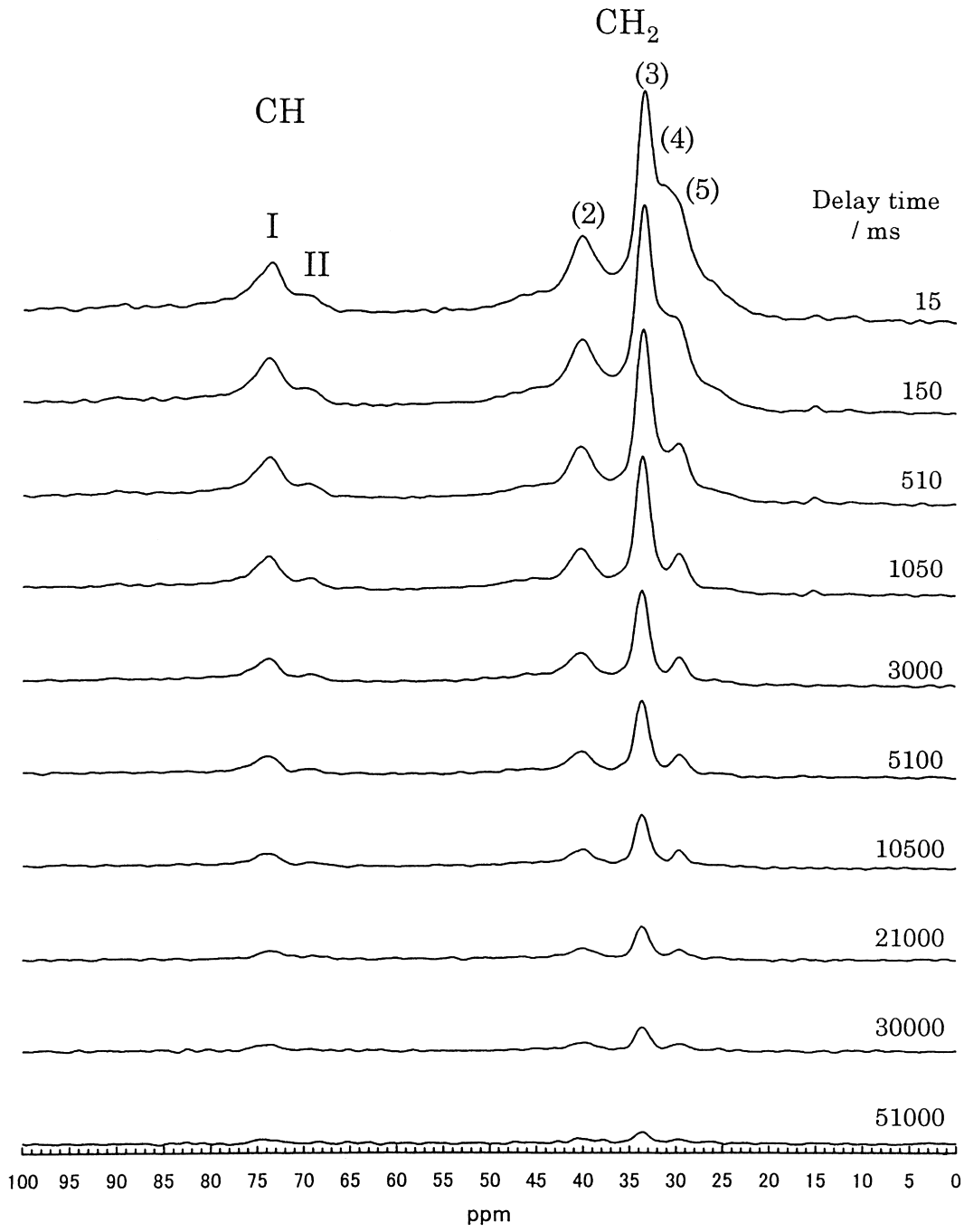

Fig. 8. Partially-relaxed 67.8 MHz ^{13}C NMR spectra of EVOH with the ethylene content of 74% in the solid-state using the Torchia pulse sequence.

hydrogen bond. In the VVV sequence the *mm* triad will be able to form two intramolecular bonds and/or one intramolecular hydrogen bond, but the *rr* triad cannot form an intermolecular hydrogen bond. The formation of hydrogen bonds is largely affected by the stereochemical structure.

Further, when the exact assignment of these spectra is performed, we must take into account the effect of the triad configurations in the EVE and EVV sequences in addition to the effect of the triad configurations in the VVV sequence on the ^{13}C chemical shift behavior. In the EVE sequence, the V unit forms one intermolecular hydrogen bond or no hydrogen bond is formed. In the EVV sequence, the VV unit can take two kinds of *m* and *r* configurations, which are represented by VV(*m*) and VV(*r*), respectively. It is considered that the central V unit in the EVV(*m*) sequence can take three kinds of hydrogen-bonded structures such as one intramolecular hydrogen bond and one intermolecular hydrogen bond, one intramolecular hydrogen bond or one intermolecular hydrogen bond, and no hydrogen bond. On the contrary, it is considered that the central V unit in the

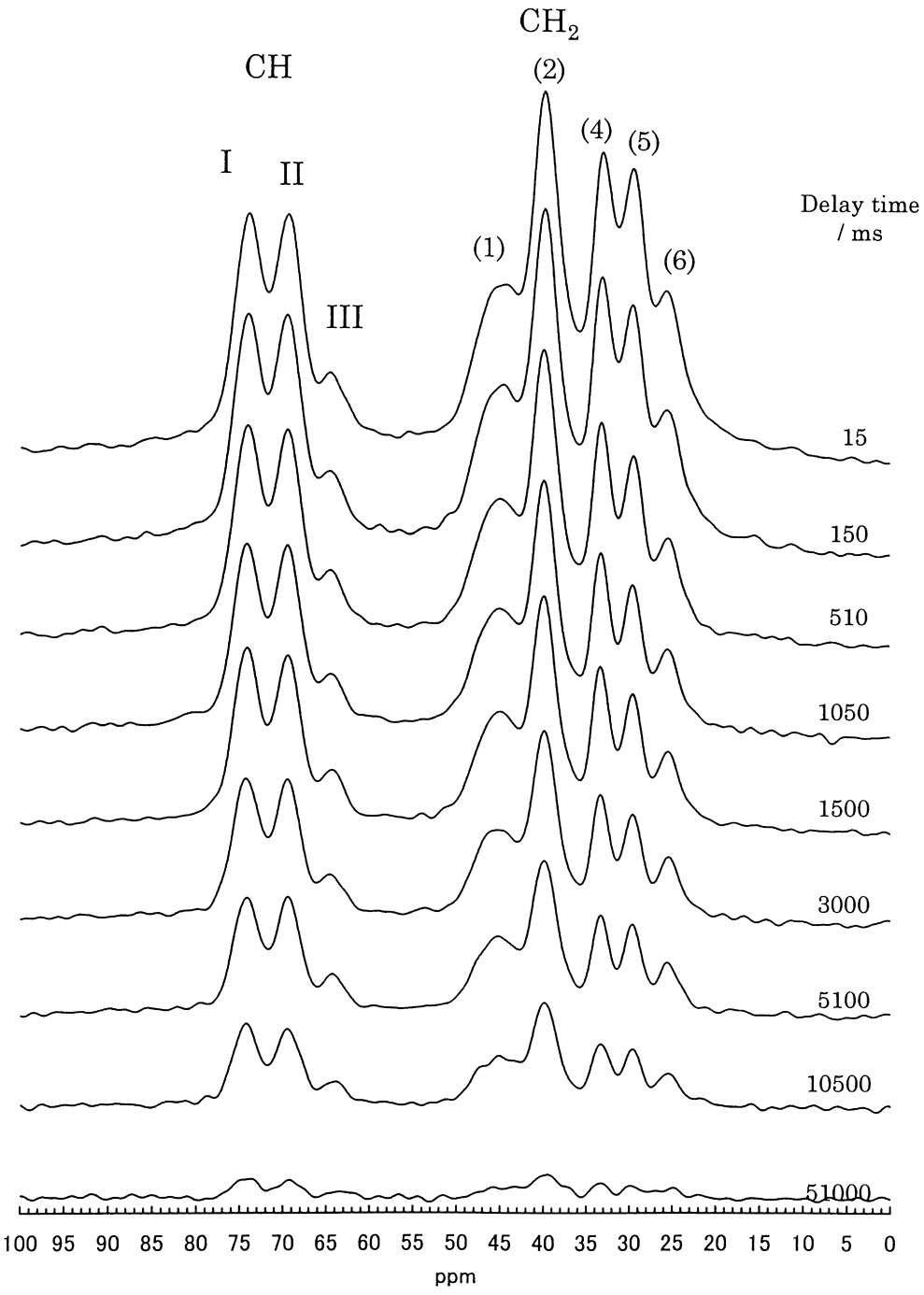

Fig. 9. Partially-relaxed 67.8 MHz ^{13}C NMR spectra of EVOH with the ethylene content of 48% in the solid-state using the Torchia pulse sequence.

EVV(*r*) sequence can form either one intermolecular hydrogen bond or no hydrogen bond. The frequency number of V unit sequences $\gtrsim 2$ is increased as the ethylene content is increased from 0 to 40% (Fig. 2), and then the fractions of the EVV(*m*) and EVV(*r*) sequences are increased. From these results, the EVV(*m*) sequence may be assigned to peak I′.

In paraffins and polyethylene, the ^{13}C chemical shift behavior is sensitively affected by the conformation, that is whether the C–C bond takes the *trans* (*T*) conformation or *gauche* (*G* or *G*′) conformation. The ^{13}C chemical shift of the CH_2 carbon in the *gauche* conformation relative to the CH_2 carbon three bonds away, moves upfield by about 5.3 ppm compared with that in the *trans* conformation [21,22]. This is the so-called *γ-gauche*-effect [23]. If fast exchange occurs between the *trans* and *gauche* conformations on the NMR timescale, the observed chemical shift becomes a statistical-weight average over the chemical shifts for the *trans* and *gauche* conformations. Thus, the averaged chemical shift moves downfield by about 3 ppm

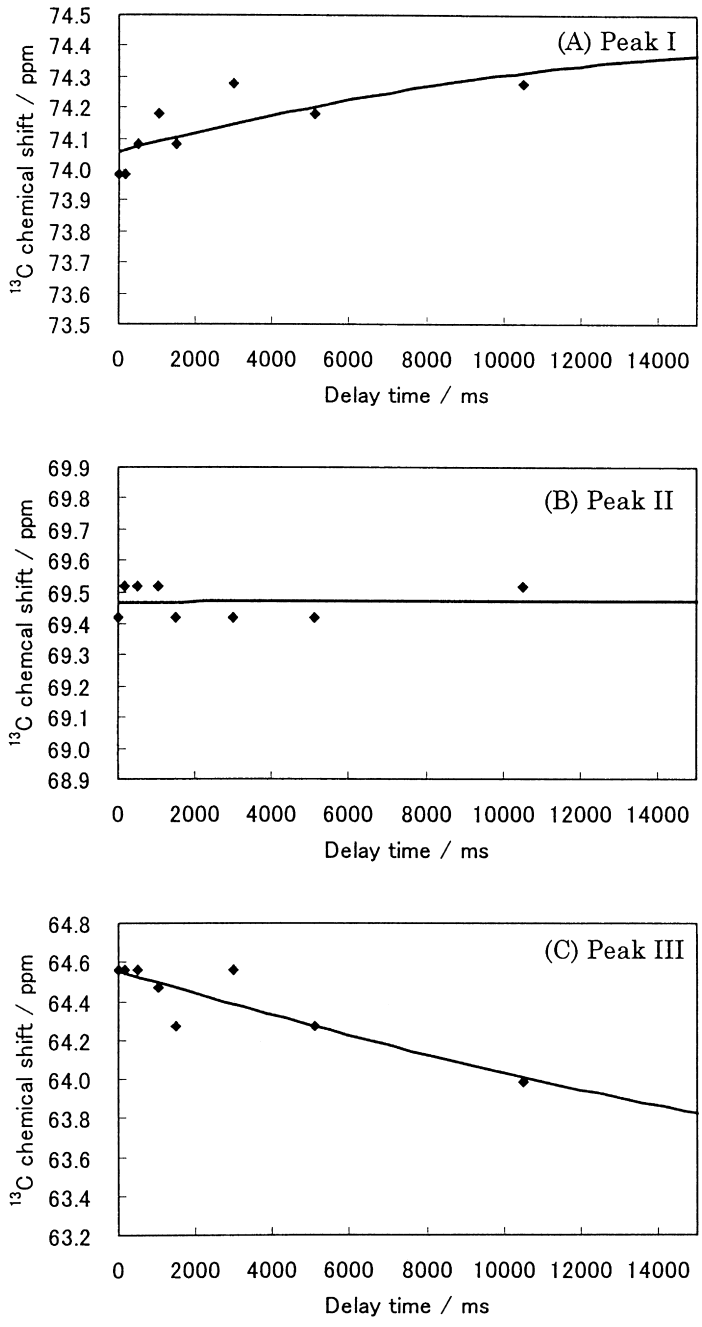

Fig. 10. Plots of the ^{13}C chemical shifts of peaks I, II and III of the CH carbon for solid EVOH with the ethylene content of 48% against the delay time in the Torchia pulse sequence. (A): peak I; (B): peak II; and (C): peak III.

relative to that in the *trans* conformation by using the statistical-weight that the conformational energy for the *trans* conformation is more stable by 600 cal/mol than that for the *gauche* conformation [10]. Naturally, this effect must be taken into account when making the peak assignment.

The ^{13}C signal of the CH carbon of the central V unit in the EVE sequence of EVOH in dimethylsulfoxide solution appears at about 69.5 ppm. In the solution-state, the E units are undergoing fast exchange between the *trans* and *gauche* conformations. On the contrary, in the solid-state the E units predominantly take the *trans* conformation. For this, it is predicted that in the solid-state the CH carbon of the V unit has no γ-*gauche*-effect from the CH_2 (1) carbon of the left side E unit and CH_2 (2) carbon neighboring the right side E unit as indicated by $-CH_2(1)-CH_2-CH_2-CH(OH)-CH_2-CH_2-CH_2(2)-$, and hence the ^{13}C chemical shift moves downfield by about 3 ppm relative to the observed chemical shift in the solution-state. Thus, the CH carbon of the V unit in the solid-state is predicted to appear at about 72.5 ($= 69.5 + 3$) ppm. Further, the hydrogen bonding effect must be taken into account in the ^{13}C chemical shift calculation, as discussed above, and the formation of one

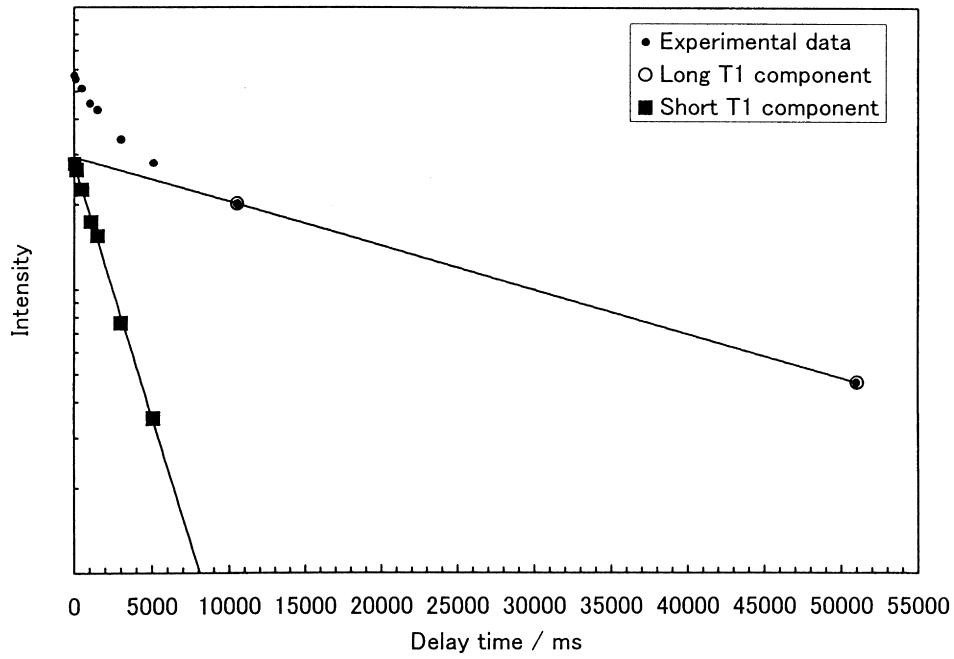

Fig. 11. Plots of the ^{13}C T_1 decay of peak I of EVOH with the ethylene content of 48% against the delay time in the Torchia pulse sequence.

hydrogen bond lead to a downfield shift of 6 ppm. Thus, the ^{13}C signal of the CH carbon in the solid-state is predicted to appear at 72.5–78.5 ppm (which is averaged to be ca. 76 ppm). This is close to the ^{13}C chemical shift position (about 77 ppm) of peak I corresponding to the CH carbon of solid PVA. Therefore, it can be said that the peak of the CH carbon of the central V unit in the EVE sequence may overlap with peak I which comes from the CH carbon in the VVV sequence with two hydrogen bonds. Consequently, if the ethylene content is increased, the fraction of the EVE sequence is increased and so the intensity of peak I is correspondingly increased. It is apparent that peak I moves upfield with an increase in the ethylene content.

The intensity of peak I for EVOH with low ethylene content is much smaller than that of peak II (Fig. 3). However, the intensity of peak I for EVOH with high ethylene content is increased and peak I appears clearly. As the ethylene content is increased, the number-average sequence length of the V unit decreases and the number of EVEs with a sequence length of one is increased as shown in Figs. 1 and 2. From these results, it can be said that as the ethylene content is increased, the fraction of peak I is increased and the fractions of peaks II and III are decreased.

It is known that the breakdown of hydrogen bonding and the stretching of a hydrogen-bonded length lead to an upfield shift of the carbon associated with it. Therefore, it can be considered that the observed upfield shift comes from a change of the hydrogen-bonded structure. As seen from the above experimental results, an increase of the ethylene content leads to a decrease in the average sequence length of the V unit in EVOH, and the fraction of isolated consecutive V units with two hydrogen bonds is increased.

On the basis of these results, we are concerned with the origin of the upfield shift of peaks I and II with an increase in ethylene content. It can be assumed that the hydrogen bond strength in solid EVOH is not so strong when compared with that in solid PVA. This comes from the fact that as the ethylene content is increased, an average sequence length of the V unit becomes short and hence the intermolecular interaction by the formation of consecutive hydrogen bonds becomes weak, and in addition the existence of the noncrystalline component of the ethylene units, in which the CH_2 carbons are undergoing fast exchange between the *trans* and *gauche* conformations. Such a situation may lead to an exchange between the –CH–OH···OH–CH– (hydrogen bonded) and the –CH–OH + –CH–OH (not hydrogen bonded) structures. Thus, the observed ^{13}C chemical shift (δ_{obs}) is expressed by

$$\delta_{obs} = (1 - \alpha)\delta_{OH+OH} + \alpha\delta_{OH\cdots OH} \quad (1)$$

where $\delta_{OH\cdots OH}$ and δ_{OH+OH} are the ^{13}C chemical shifts of the CH carbons with and without a hydrogen bond, respectively, and α is the fraction of the hydrogen-bonded CH carbon. The $\delta_{OH\cdots OH}$ appears at a lower field than the δ_{OH+OH}. This equation shows that as $\delta_{OH\cdots OH}$ is much larger than δ_{OH+OH}, the observed ^{13}C signal moves upfield with a decrease in α. In EVOH with low ethylene content, the T_g is above the measurement temperature (about 45°C) (Table 2). Thus, the measurement temperature is below T_g. For this, the V units are frozen in molecular motion on the NMR timescale. This leads to high CP efficiency in the ^{13}C CP/MAS NMR experiment. With an increase in the ethylene content, the T_g value of EVOH is decreased, and the measurement temperature becomes above T_g. The V units

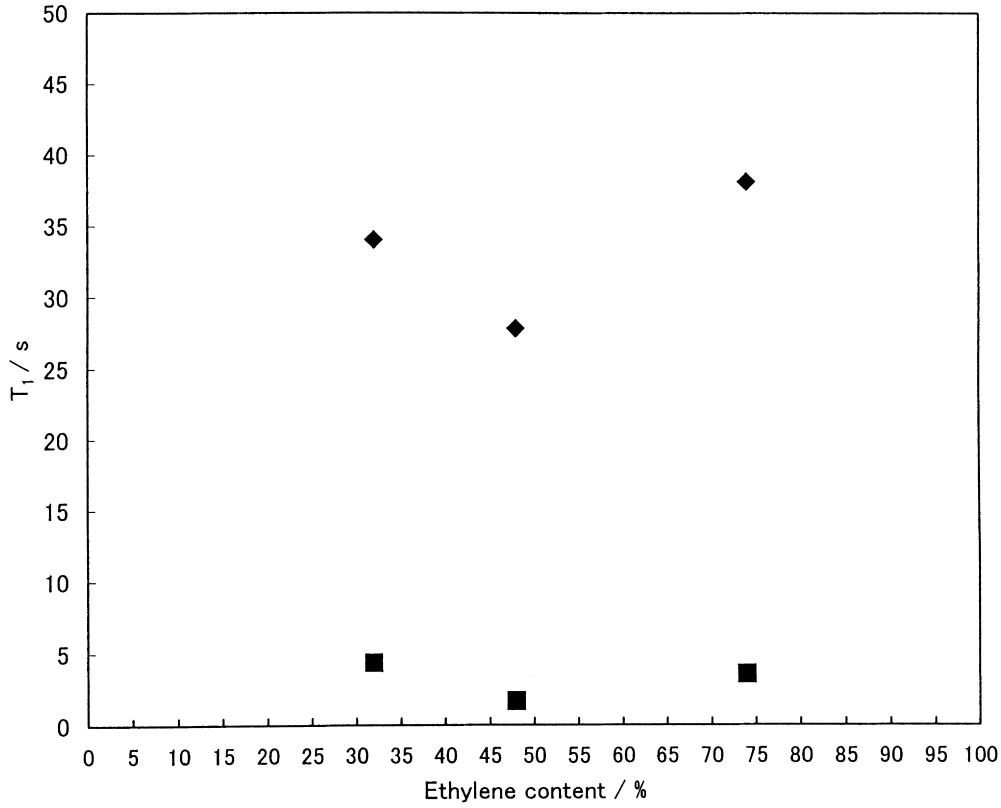

Fig. 12. Plots of the ^{13}C T_1 of peak I of EVOH samples against the ethylene content. ◆:long T_1 component; and ■:short T_1 component.

begin to undergo molecular motion. Then, the breakdown of the hydrogen bond may be induced and, then, its fraction $(1-\alpha)$ is increased.

Next, we are concerned with the peak assignment of the CH_2 carbon in the E and V units in EVOH. By using reference data of polyethylene and paraffins, and PVA in the solution- and solid-states, the CH_2 carbons with asterisks in $-CH_2-CHOH-CH_2{}^*-CHOH-CH_2$(1), $-CH_2-CHOH-CH_2{}^*-CH_2-CH_2-$(2), $-CH_2-CHOH-CH_2{}^*-CH_2-CH_2-$(3), $-CH_2-CH_2-CH_2{}^*-CH_2-CH_2-$ (4), $-CHOH-CH_2-CH_2{}^*-CH_2-CH_2-$ (5) and $-CHOH-CH_2-CH_2{}^*-CH_2-CHOH-$ (6) appear at about 45, 40, 33, 30, 29 and 25 ppm, respectively. In polyethylene, peaks at about 30 and 33 ppm are assigned to the CH_2 carbons for the noncrystalline component in which the CH_2 units are undergoing a fast exchange between the *trans* and *gauche* conformations, and for the crystalline component in which the CH_2 units take the *trans* zigzag conformation, respectively [24]. It is reported from the solid-state NMR study on melt-quenched polyethylene samples that at room temperature the fractions of the crystalline and noncrystalline components are estimated to be about 70 and 30%, respectively [10]. Therefore, peaks (3) and (4) at about 33 and 30 ppm as shown in Fig. 3 come from both the $-CHOH-CH_2-CH_2{}^*-CH_2-CH_2-$ unit and $-CH_2-CH_2-CH_2{}^*-CH_2-CH_2-$ unit without and with fast exchange between the *trans* and *gauche* conformations, respectively. Fig. 7 shows the ^{13}C PST/MAS NMR spectra of the solid EVOH sample with an ethylene content of 74%. In these spectra, the mobile component is enhanced by the PST/MAS method. As shown in Fig. 7(a) in the EVOH with an ethylene content of 74%, the peak at about 30 ppm is enhanced. This is because the T_g value of the EVOH sample is below the measurement temperature (about 45°C) and the T_g value of EVOH with an ethylene content of 34% is about 65°C and so the measurement temperature is below T_g. The intensity of the peak in the vicinity of about 30 ppm is enhanced. From such a situation, it can be understood that the intensity of the peak in the vicinity of about 30 ppm decreases with an increase in the ethylene content, because of the reduction of the CP efficiency which comes from the enhancement of the molecular mobility and also a decrease of its sequence fraction.

3.3. Dependence of the ^{13}C T_1 of EVOHs on the ethylene content

Figs. 8 and 9 show partially relaxed ^{13}C spectra of solid EVOHs with ethylene contents of 74 and 48%, respectively, by using the Torchia pulse sequence. In these ^{13}C T_1 experiments, the mobile component with a short T_1 value disappears at short delay time. On the contrary, the immobile component with a long T_1 value remains for long delay time.

Fig. 10 shows the plots of the ^{13}C chemical shifts for peaks I and II, III against the delay time in the partially relaxed ^{13}C NMR experiments. As the delay time becomes longer, the chemical shift position of peak I moves downfield.

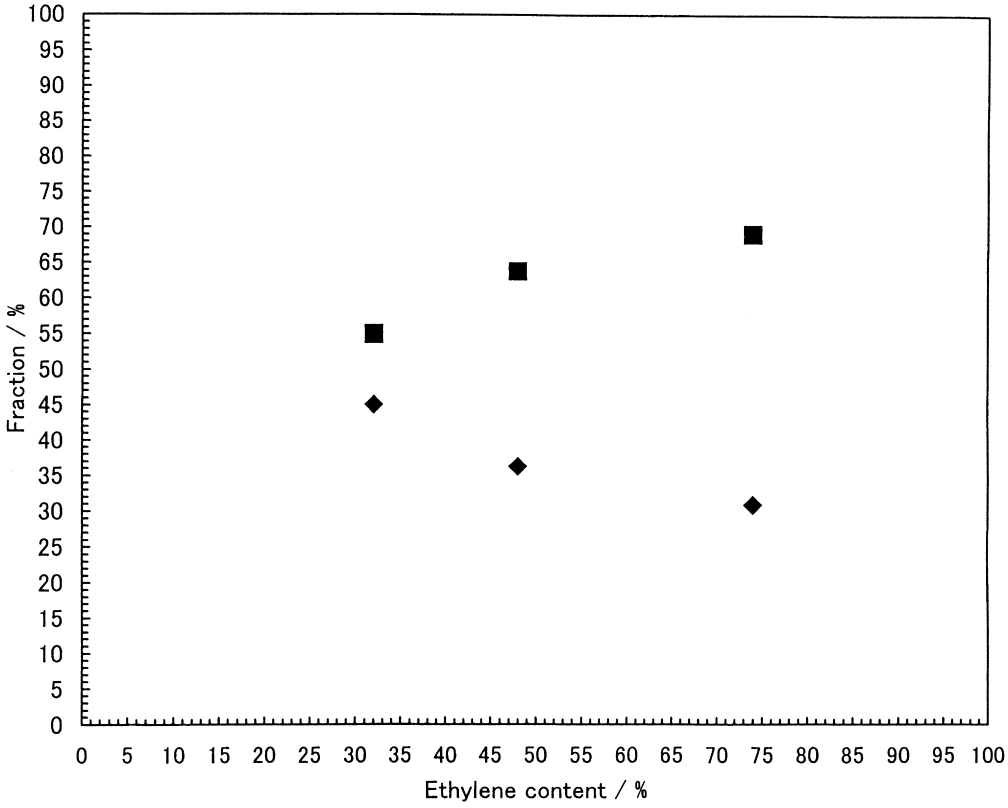

Fig. 13. Plots of the fraction of the ^{13}C T_1 of peak I of EVOH samples against the ethylene content. ◆: long T_1 component; and ■: short T_1 component.

The long T_1 component appears at a lower field than the short T_1 component. From these experimental results, it can be said that the EVE peak of the mobile component contributing to peak I appears at a higher field than the immobile component contributing to peak I (corresponding to a VVV unit with two hydrogen bonds).

In order to clarify the mobility of the individual signals of the EVOH sample with an ethylene content of 48% (T_g = 50°C) at 45°C as a typical example, the intensities of the peaks were plotted against the delay time as shown in Fig. 11. It is apparent that peak I has two components with different mobilities. As it is considered that the molecular motions for these components are in the slow motion region ($\omega\tau_c > 1$, where ω is the resonance frequency and τ_c the correlation time in molecular motion) in the BPP theory [25], the long T_1 component and the short T_1 component are assigned to strongly restrained and weakly restrained components in molecular motion, respectively. The plot of the ^{13}C T_1 values for these two components of peak I for EVOH samples with a wide range of ethylene contents against the ethylene content is shown in Fig. 12. It is found that the T_1 values of the two components are almost independent of the ethylene content. The fractions of these two components are plotted against the ethylene content as in Fig. 13. As the ethylene content increases, the short T_1 component increases, and the long T_1 component decreases. From these results, the long T_1 component can be assigned to the VVV unit forming two hydrogen bonds, which lead to a strong restraint in molecular motion, and the short T_1 components can be assigned to the EVE unit with one hydrogen bond or no hydrogen bond which lead to a weak restraint in molecular motion.

As for the CH_2 carbon, the peak at 30 ppm delays faster compared with the peak at 33 ppm (Fig. 8). The peak at 30 ppm in EVOH with high ethylene content disappears at short delay times (Figs. 8 and 9). This arises from the fact that the CH_2 carbons with the *trans* zigzag conformation in the crystalline component, which appear at 33 ppm, are frozen in molecular motion on the NMR timescale, and the CH_2 carbons in the noncrystalline component, which appear at about 30 ppm, are undergoing fast exchange between the *trans* and *gauche* conformations.

Finally, we can draw the following conclusions. The solid-state ^{13}C NMR spectral assignment for EVOH samples in the solid-state with a wide range of ethylene contents was successfully performed. The structure and dynamics of EVOHs with changes of ethylene content were elucidated.

References

[1] Ketels H. Macromolecules 1988;21:2032.
[2] Ketels H, Haan Jde, Aerdts A, Velden G. Polymer 1990;31:1419.
[3] VanderHart DL, Simmons S, Gilman JW. Polymer 1995;36:4223.

[4] Ando I, Asakura T, editors. Solid state NMR of polymers. Amsterdam: Elsevier, 1998.
[5] Terao T, Maeda S, Saika A. Macromolecules 1983;16:1535.
[6] Horii F, Hu S, Ito T, Odani H, Kitamura R. Polymer 1992;33:2299.
[7] Kobayashi M, Ando I, Ishii T, Amiya S. Macromolecules 1995;28:6677.
[8] Kobayashi M, Ando I, Ishii T, Amiya S. J Mol Struct 1997;417:238.
[9] Kanekiyo M, Kobayashi M, Ando I, Ishii T, Amiya S. J Mol Struct 1998;447:49.
[10] Ando I, Yamanobe T, Akiyama S, Okamoto T. Solid State Commun 1987;62:785.
[11] Schaefer J, Stejskal EO. Top Carbon-13 NMR Spectrosc 1980;3:283 for example.
[12] Yannoni CS. Acc Chem Res 1982;15:201.
[13] Wasylishen RC, Fyfe CA. Annu Rept NMR Spectrosc 1982;12:1.
[14] Fujito T, Deguchi K, Ohuchi M, Imanari M, Albright MJ. The 20th Meeting of NMR, Tokyo. 1981:68.
[15] Akieda T, Mimura H, Kuroki S, Kurosu H, Ando I. Macromolecules 1992;25:5794.
[16] Tochia DA. J Magn Reson 1978;30:613.
[17] Bruck MD. Macromolecules 1988;21:2707.
[18] Cheng HN, Lee GH. Macromolecules 1988;21:3164.
[19] Moritani T, Iwasaki H. Macromolecules 1978;11:1251.
[20] Bovey FA. Polymer conformation and configuration. New York: Academic Press, 1972.
[21] Ando I, Yamanobe T, Sorita T, Komoto T, Sato H, Deguchi K, Imanari M. Macromolecules 1984;17:1955.
[22] Chen Q, Yamada T, Kurosu H, Ando I, Shiono T, Doi Y. J Polym Sci 1992;B30:591.
[23] Tonelli AE, Shilling FC. Acc Chem Res 1981;14:233.
[24] Earl WL, VanderHart DL. Macromolecules 1979;12:762.
[25] Bloembergen N, Purcell EM, Pound RV. Phys Rev 1948;73:679.